Annals of Science and Technology - A, Vol 7 (2): 69-75, 2022
Copyright: An Official *Journal* of the Nigerian Young Academy
ISSN: 2 544 6320

sciendo

ARTICLE

Adsorption Study of Paracetamol with Graphene oxide Synthesized from Agricultural waste

Temitope M. Osobamiro[1*] and Adewale Oladipo[1]

[1]Department of Chemical Sciences, Faculty of Science, Olabisi Onabanjo University, Ogun State, Nigeria

Received 2nd th August 2022, Accepted 5th December, 2022
DOI: 10.2478/ast-2022-0011

**Corresponding author*
Temitope M. Osobamiro E-mail: osobamiro.temitope@oouagoiwoye.edu.ng, Tel: +2348056628102

Abstract

The production of cheap and eco-friendly graphene material for the removal of contaminants in wastewater is necessary for sustainable water treatment. In this study, the production of graphene oxide from agricultural wastes (rind of orange and palm kernel shell) for the adsorption of paracetamol from aqueous solution was examined. The Graphene Oxides (GO) were produced using modified Hummer method and characterized using XRD and FTIR analyses. The kinetic data were analyzed using the pseudo-first and pseudo-second order equations, while the equilibrium isotherm data were fitted into Langmuir and Freundlich isotherms. FTIR spectral indicated mainly the presence of oxygen containing functional groups such as Hydroxyl group (OH) and Carbonyl group (C=O, C-O) confirming the synthesis of graphene oxide. The highest percentage removal of 76.6 from the aqueous paracetamol solution was established at pH 7, adsorbent dose of 0.4 g and contact time of 80 minutes with graphene oxide from palm kernel shell. The adsorption data was best described by pseudo-second-order model (R2> 0.900) and Freundlich isotherm. Therefore the rind of orange and palm kernel shell can be suitable cheap alternatives to graphite for the synthesis of GO. Modification and further purification of the GO can be carried out to enhance their adsorption capacities.

Keywords: Pharmaceuticals, agricultural waste, graphene oxide, adsorption, paracetamol, wastewater

BY-NC-ND © *Osobamiro and Oladipo*. This work is licensed under the **Creative Commons Attribution-Non-Commercial-NoDerivs License 4.0**

1.0 Introduction

Pharmaceutical wastes are unregulated emergent contaminants that are indiscriminately released into water bodies causing pollution (Al-Khateeb et al., 2014, Tijani et al., 2016, Barroso et al., 2019). These include: wastes from drug production processes, expired drugs, incomplete metabolized drugs in the body which are usually disposed into water bodies (Al-Khateeb et al., 2014, Tijani et al., 2016, Rivera-Utrilla et al., 2013). Photocatalysis, nanofiber-membrane, precipitation, electro-coagulation, flotation, chemical oxidation, filtration, ion-exchange, and adsorption are some of the treatment techniques that have been used for the removal of pharmaceuticals waste in wastewater (Homem and Santos, 2011; Rivera-Utrilla et al., 2013). Of all these techniques, adsorption has been found to be the most promising process for wastewater remediation.

Many carbon materials such as activated carbon, Fullerenes, biochar,grapheme, have been used as adsorbent, most of which are either expensive or havelow efficiency for the removal of pharmaceuticals in wastewater (Li et al., 2013; Rivera-Utrilla et al., 2013; Al-Khateeb et al., 2014; Mukoko et al., 2015).

Nowadays, graphene-based adsorbent materials with unique characteristics e.g. good dispersion in water, large delocalized π-electron system, high adsorption capacity, larger specific surface area and high selectivity, have been found to be a better adsorbent (Wang et al., 2013; Sui et al., 2016). Also, hydroxyls, ketones, epoxides and carboxyl functional groups present on GO makes it an excellent binder for organic groups (Liu et al., 2013; Li et al., 2015). High cost of commercial graphene oxide has made researchers to switch to carbonaceous materials from agricultural wastes as alternate precursors for the synthesis of graphene (Somanathan et al., 2015; Aro-modiu et al., 2019). Agricultural wastes are usually discarded in the environment or oftentimes burn openly causing adverse effects to the environment. Graphene and GO have been successfully produced from agricultural wastes including: sugarcane bagasse (Somanathan et al., 2015, Debbarma et al., 2020), groundnut and almond shells (Aro-modiu et al., 2019), rice straw, mature beech pinewood sawdust (Tohamy et al., 2020), coconut husk (Grace and Malar, 2020) and tea waste (Amir Faiz et al., 2020). Nasir et al. (2017) used the new method of Marcano et al. (2010) to produce reduced graphene oxide (rGO) from graphene oxide (GO) using various oil palm wastes such as oil palm leaves, palm kernel shells, and empty fruit bunches. Graphene oxide had been used as excellent adsorbents for the removal of the pharmaceuticals from aqueous solutions; these include aspirin, acetaminophen, and caffeine (Al-Khateeb et al., 2014), sulfamethoxazole and ciprofloxacin (Chen et al., 2015), tetracycline (Yuan et al., 2012) and acetaminophen and aspirin (Akpotu and Moodley, 2018).

The present study was aimed at addressing the challenges of agricultural waste disposal and remediation of contaminants by synthesizing GO using the modified Hummer method from rind of orange and palm kernel shell for the removal of paracetamol from aqueous solution.

2.0 Experimental

2.1 Sample collection and reagents

Agricultural wastes samples [rind of orange (B) and palm kernel shell (C)] were collected from a major market in Ijebu-Ode and at a palm oil production plant in Ijebu-Igbo, Ogun State respectively. The two samples were thoroughly washed, rinsed with tap water, and air-dried to prevent loss of carbon content during oven-drying for two weeks before use. Reagents used were of analytical grade purchased from Sigma Aldrich and they included: Paracetamol [N-(4-hydroxyphenyl) ethanamide] standard, iron (III) chloride hexahydrate ($FeCl_3.6H_2O$), hydrochloric acid (HCl), sodium nitrate, tetraoxosulphate(VI) acid (H_2SO_4), hydrogen peroxide (H_2O_2), potassium tetraoxomanganate(VII) [$KMnO_4$].

2.2 Carbonization and synthesis of graphene oxide

The two samples (B and C) were carbonized in a furnace at 300 ºC for 24 hours, crushed into fine powder with mortar and pestle and stored in an air tight container. Graphite was synthesized from the carbonized materials using modified Hummer method as reported by Aro-modiu et al. (2019) and Akhavan et al. (2014). Two grams (2 g) of the carbonized material and 1 g of FeCl3.6H2O were added to 250 cm3 of distilled water in a conical flask to produce graphite. This was grinded into powdery form and later converted to graphene oxide (GO) as reported by Aro-Modiu et al. (2019). The percent ratio of the weight of the desired product yield was then calculated using equation 1

$$Percentage\ yield = \frac{weight\ of desired\ product}{weight\ of starting\ material} \times 100\% \quad [1]$$

2.3 Characterization of the synthesized materials

The synthesized GO sorbents were characterized using Fourier Transform Infra-Red (FTIR) spectrophotometer and X-Ray Diffractometer (XRD). The FTIR analysis was done to identify the functional groups present, while crystalline features of the graphene oxides produced were obtained by running the samples through the Rigaku D/Max- IIIC X-ray diffractometer with a scanning rate of 2o/min from 2 to 50oat room temperature, with a CuKα radiation set at 40kV and 20Ma. The FT-IR spectral analysis was run as KBr pellets in the frequency range of 4000 - 500 cm-1on FT-IR (Shimadzu FT-lR 8400s) spectrophotometer and the results obtained were compared with conventional GO.

2.4 Adsorption study of graphene oxide

Adsorption study was carried out using the produced GO in the removal of paracetamol from aqueous solution under the following reaction conditions: time (0 min to 200 min), adsorbent mass (0.4 g), adsorbate (20 mg/L), solution pH (7 and 10), and solution temperature (298 K). The pH of the mixture was adjusted using 0.1 M NaOH/0.1M HCl solutions. The solution was shaken continuously for 10 minutes, centrifuged at 6000 rpm and filtered through a 0.45 mm cellulose acetate filter to avoid blockage of the High-Performance Liquid Chromatography (HPLC) column by the graphene oxide particles. The concentration of residual paracetamol in the supernatant was determined using HPLC (Chen et al., 2015). The percentage adsorption in solution was calculated using the equation:

$$\text{Removal efficiency } (\%) = \frac{(A-B)}{A} \text{x } 100 \quad [2]$$

where A is the initial concentration (mg/L), B is the final concentration (mg/L) after a certain period of the time (min).

2.5 Determination of the concentration of paracetamol using HPLC

The concentration of paracetamol remaining after adsorption was determined using HPLC (Cecil Instrument ACE-121-1546) with UV detector after calibration. Separations were achieved on analytical reversed phase C18 column (ACE 5,150 x 4.6 mm 1.d) at a mobile phase flow rate of 1mL /min under isocratic conditions (a mixture of water/methanol/glacial acetic [70: 27: 3]). The sample size injected was 20 µL and UV detection wavelength was 275nm.The chromatographic run time was 20 mins and its retention time was 6.41mins.

3.0 Results and Discussion

3.1 Percentage yield of graphene oxide from carbonized materials

The % yield of GO produced using B and C as precursors were calculated using equation 1 and the results are presented in Table 1. Figures 1B and 1C give the percentage yield of graphite powder produced from the raw carbonized materials while Figures 2B and 2C showcase the percentage yield of GO produced from the conversion of graphite powder produced in previous step to GO. Palm kernel seed waste (C) gave more yield of GO compared to rind of orange waste (B).

3.2 Result of characterization of the produced graphene oxide

The X-ray diffraction (XRD) is the most widely used technique for general crystalline material characterization. This technique was applied in this study to authenticate and validate that the synthesized product was GO. The appearance of a slightly sharp peak in the region of 2 θ~ =130for the basal reflection (220) with a d-spacing of 0.617 nm for B and sharp diffraction peak of CGO at 2θ ~ 110 with a d-spacing of 0.737 nm (Figure 1) confirms the oxidation of graphite and presence of graphene oxide. This d-spacing was due to the incorporation of oxygen functional groups intercalate into the

Table 1: Results of percentage yield of graphite powder produced from the powdered agricultural wastes.

Agricultural waste	Carbonized powder (g)	Graphite powder(g)	Percentage yield (%)
1B	2.0 ±0.3	1.79 ± 0.03	88.00 ± 0.03
1C	2.0 ±0.2	1.86 ± 0.02	93.00 ± 0.01
Waste	**Graphite (g)**	**GO (g)**	**% yield (%)**
2B	2.0 ±0.2	1.20 ±0.01	60.00 ± 0.10
2C	2.0 ±0.1	1.59 ±0.01	79.5 ± 0.10

Table 2: Adsorption kinetics parameters for Ist and 2nd order models

Model	Parameter	pH10		pH 7	
		B	C	B	C
First-order	qe	4.055	3.148	6.295	6.471
	Ki	0.000	0.002	0.005	0.005
	R^2	0.801	0.561	0.439	0.447
Second-order	qe	14.700	14.290	4.484	3.876
	Ki	0.039	0.029	0.018	0.018
	R^2	0.999	0.999	0.984	0.981

Table 3: Adsorption parameters for Langmuir and Freundlich models

Isotherm	pH 7		pH 10	
Langmuir model	B	C	B	C
qL (mg/g)	0.542	0.584	0.246	0.167
KL (L/g)	0.177	0.191	0.083	0.773
R^2	0.840	0.837	0.983	0.975
Freundlich model				
K_F(mg/g) (mg/L)$1/n$	15.1	130.3	29.58	22.4
n	0.838	0.928	0.288	0.234
R^2	0.825	0.809	0.992	0.989

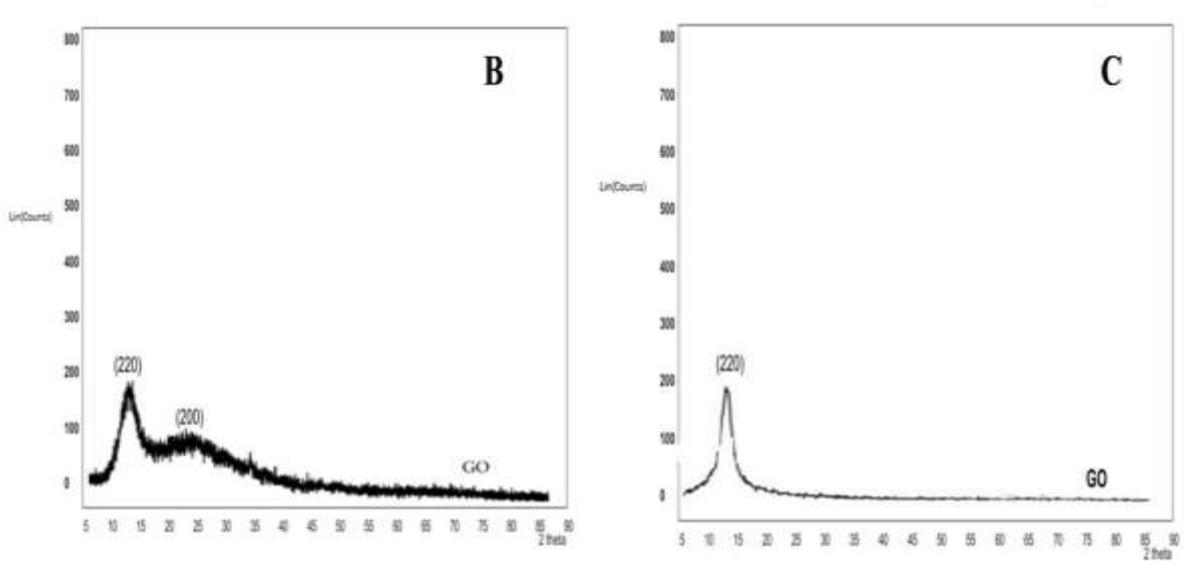


Figure 1: XRD pattern of Graphene oxide from B and C.

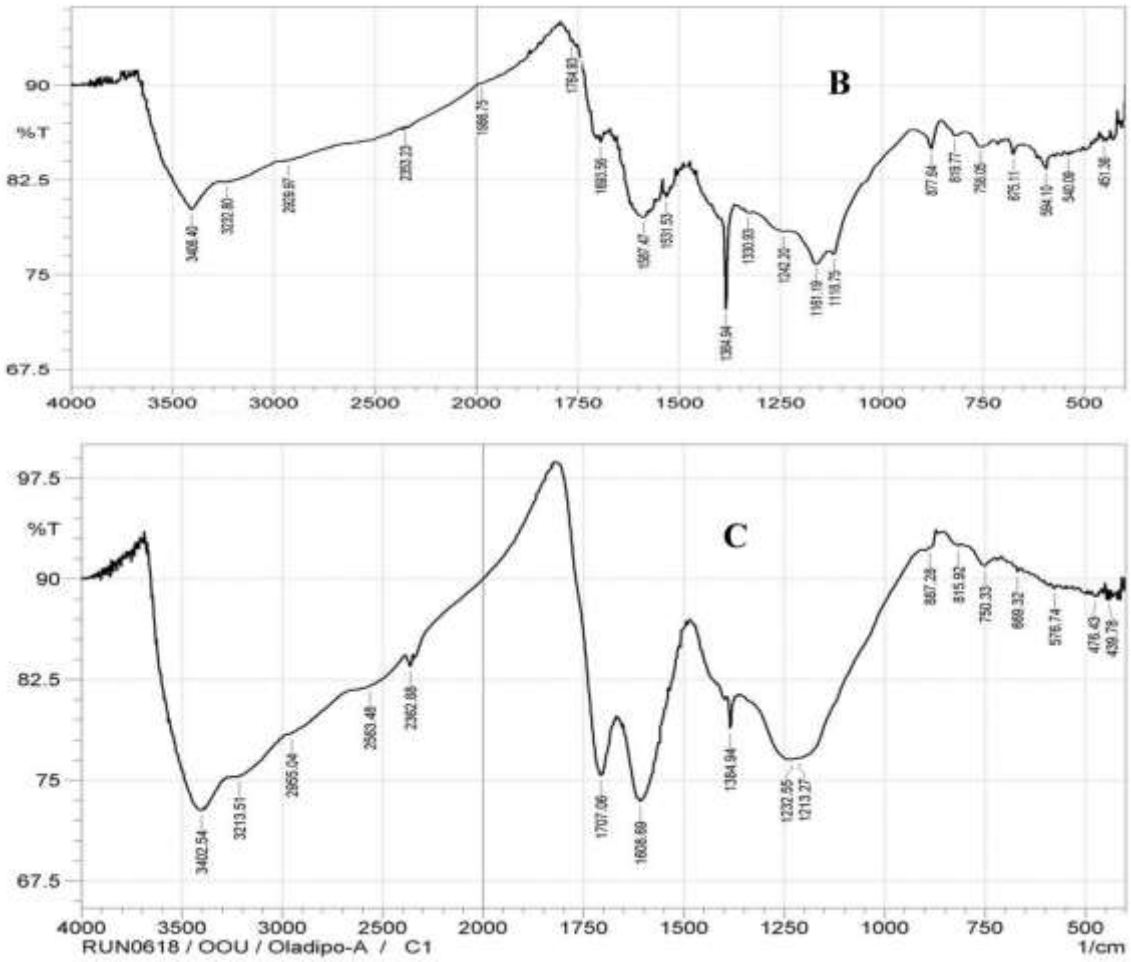


Figure 2: FT-IR spectrum of graphene oxide from B and C.

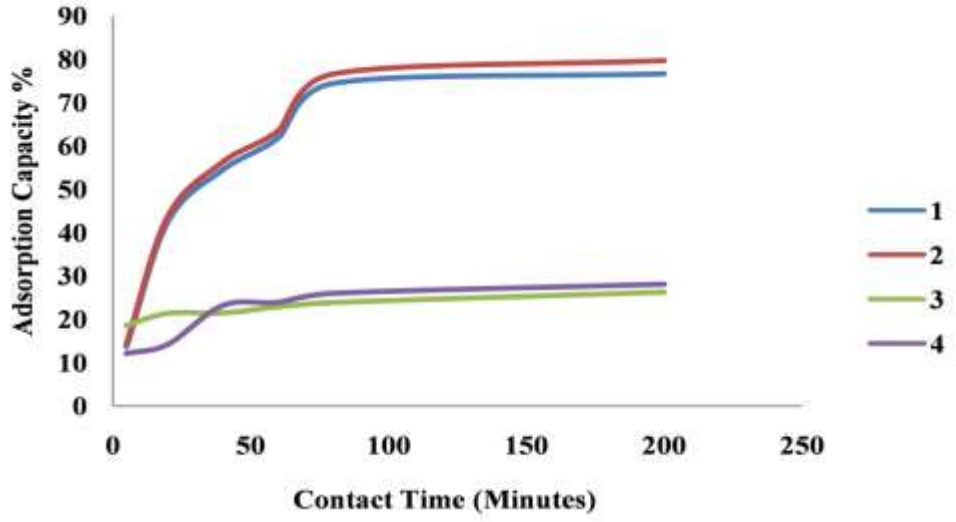


Figure 3: Effect of contact time on percentage adsorption capacity of paracetamol standard at pH 7 (1 and 2) and 10 (3 and 4) unto B and C respectively.

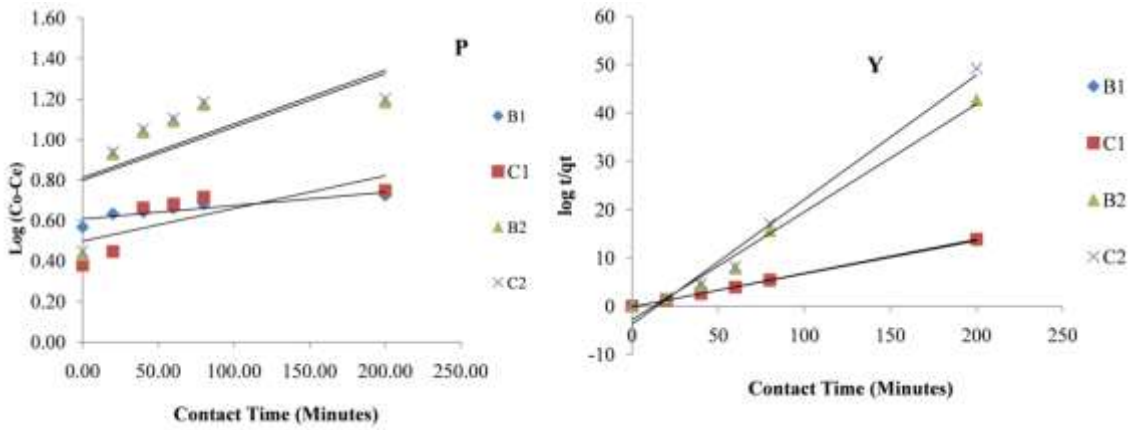


Figure 4: Pseudo-first order adsorption (P) at pH 10 (B1 & C1) and 7 (B2 & C2), and pseudo-second order adsorption kinetics (Y) at pH 10 (B1 & C1) and 7 (B2 & C2).

interlayer of the graphite sheets. The significant increase in d-spacing can be attributed to oxygen functional groups intercalate into the interlayer of the graphite sheets. This is similar to the peak at 2θ ≈ 11.60 recorded by earlier workers (Somanathan et al., 2015; Alam et al., 2017; Grace and Malar, 2020). All of these confirmed that the synthesized products are graphene oxide. There are also diffraction peaks at 2θ ~ 25.50 which may be due to partial reduction of part of the GO to reduced GO, as reported by Nasir et al. (2017).

The FT-IR spectra of GO shown in Figure 2 (B & C) confirm the presence of oxygen containing hydroxyl, epoxy and carboxylic groups upon oxidation of the graphite obtained from agro-waste. This is similar to the reports of previous studies (Somanathanet al., 2015; Alam et al., 2017; Grace and Malar, 2020; Tohamy et al., 2020).
Figure 2 (B & C) shows the FT-IR spectrum of GO from palm kernel shell with several peaks. The peaks at 2955 cm^{-1} and 2929 cm^{-1} are characteristic of C-H stretching mode. The synthesized GO has a peak at 1167 cm^{-1} and 1118 cm^{-1} found in B (Figure 2) which can be attributed to the C-O (epoxy bond), confirming the presence of oxide or epoxy functional groups after the oxidation process while the band at 1242.20 cm^{-1} and 1232.55 cm^{-1} (Figure 2 B & C) are attributed to the C-OH group. The peaks between 1693 $cm^{-1}$and 1707 cm^{-1}(Figure 2 B & C) indicate the presence of C=O bonds (Sun et al., 2013). Significantly, the peaks at 1532$cm^{-1}$and 1587cm^{-1} in B (Figure 2) are assigned to the skeletal vibrations of un-oxidized graphitic domains. The peaks within range of 1608 and 1587 cm^{-1}in B (Figure 2) show that the C=C bond remained after oxidation process. The slightly broad peak for GO obtained from B and C at ~3406 cm^{-1} which can be attributed to the hydroxyl and carboxyl groups and residual water between the GO sheets represents the outer surface OH stretching vibration. The FT-IR spectroscopy of the two synthesized GO indicated the presence of oxygen containing functional groups (epoxy, hydroxyl, carboxylic) and these can aid Hydrogen bonding and π-π interactions (Zhang et al.,2013, Catherine et al., 2018).

3.3 Adsorption study

Adsorption study was carried out to explore the adsorption capacity of the produced graphene oxide (contact time in relation to the mass of adsorbent used). The results of effect of contact time on percentage adsorption capacity of paracetamol standard at pH 7 (B and C) and 10 (D and E) unto B and C respectively were presented in Figure 3. The adsorption of paracetamol standard increased slightly from 18.6% to 23.6% and 12.1% to 26.0% when the contact time was increased from 0 min to 80 min at pH 10 for B and C respectively whereas; at pH 7 significant increase from 13.7% to 74.4% and 14.2% to 76.6% was observed for Band C respectively.
This can be related to number of active sites available on the surface of the GO or the number of ionized paracetamol solute in the solution might have affected the adsorption process. Further increase of contact time from 80 to 200 mins, led to slight increase in the % adsorption at pH 10 and 7 (Figure 3). This can be attributed to similar effects which might have affected adsorption. From literature, GO is not surface active and dissolves in water at a higher pH (Shih et al., 2012). Therefore, low adsorption rate originated from the degree of deprotonation of the carboxyl groups on the GO at pH 10, creating a strong hydrophilicity between its basal plane and the edges (Amir Faiz et al., 2020).

Also, considering the fact that a constant concentration of GO was used for these experiments, the slow adsorption of paracetamol standard at higher contact times can be attributed to reduction in the adsorption rate driving force resulting from the decreased available sites for adsorption on the surface of GO (Wang et al., 2013, Catherine et al., 2018). Similar trends have been reported for the adsorption of different pharmaceutical standards (carbamazepine, tetracycline, ciprofloxacin and sulfamethoxazole) onto GO (Chen et al., 2015, Gao et al., 2012, Moussavi et al., 2016).

3.4 Kinetic model

The experimental data were adjusted to the pseudo-first and second order kinetic models to predict the adsorption rate and adsorption mechanism. The pseudo-first order kinetic model is expressed in equations 3.

$$\mathrm{Log}\,(qe - qt) = \mathrm{Log}qe - \left(\frac{Kit}{2.303}\right) \quad [3]$$

qt and qe are the amounts of paracetamol ions adsorbed at time t and at equilibrium in mg/g, respectively. Ki is the pseudo-first order adsorption rate constant (min−1). Figure 4 shows the plot of log (qe–qt) against contact time, the slope and intercept of the plots were used to determine the rate constant (KI) and qe, and the results are presented in Table 2. It is seen that the pseudo-first order equation did not provide a good fit to the experimental data of both the two GOs (B and C) as indicated by the low values of their linear regression [R2] (Table 2).

The pseudo-second order kinetic model assumed that chemisorption is the rate determining step and it is expressed as presented in equation 4.

$$\frac{t}{qt} = \frac{1}{K_2\,qe^2} + \frac{t}{qe} \quad [4]$$

The plot of the logarithm of t/qt versus contact time (t) is presented in Figure 4 (Y). The values of qe and K2 (equilibrium rate constant of pseudo-second order adsorption g/mg min) were calculated from the slope and intercept of the linear plot and the results are recorded in Table 2. Based on the values of the linear regression coefficients, the adsorption of paracetamol ions unto the two produced GO was found to be best described by the pseudo-second-order model (R2> 0.900) and adsorption at pH 10 performs better than pH 7. This is in agreement with the reports of earlier researchers (A-Khateeb et al., 2014; Akpotu and Moodley, 2018; Macías-García et al., 2019; Tohamy et al., 2020).

3.5 Adsorption isotherm

Adsorption isotherm expresses the relationship between the concentrations of the adsorbate removed from the liquid phase by unit mass of adsorbent at a constant temperature. This is important for prediction of adsorption parameters and contrast of adsorption performance of different adsorbent. The data for this study were fitted into Langmuir and Freundlich models and the result is presented in Table 3.

The maximum adsorption capacity of B and C at pH 7 and 10 is very low; B was ≤ 0.542mg/g and C ≤0.584 mg/g with Langmuir model. Kf and n values were calculated for Freundlich model. Large Kf values indicate a better adsorption capacity while n value corresponds to adsorbent strength and the effect of concentration on the adsorption. A value of n more than 1 represents favourable adsorption or intensity (Ismail et al., 2013). Kf and n values for C at pH 7 are the highest while others has low Kf and n values, though the n value for C at pH 7 is only closed to 1. This is in agreement with the qm value obtained for C from the Langmuir isotherm (Table 3). This indicates that C which is GO from PKS at pH 7 adsorbed a higher quantity and has higher affinity for paracetamol (Akpotu and Moodley, 2018). Going by R2 values, the adsorption of both B and C fitted well into Langmuir and Freundlich isotherms but, the adsorption study is better explain with Freundlich isotherm based on higher values of Kf and this reveals that the adsorption is mainly through parallel π–π stacking interactions and its multilayer adsorption (Catherine et al., 2018).

4.0 Conclusion

The study revealed that rind of orange and palm kernel shell indiscriminately discarded as waste can be re-utilized in the synthesis of GO. Structural characterization indicated the presence of oxygen containing functional groups (hydroxyl, epoxy and carboxylic groups) similar to the conventional GOs. Adsorption of aqueous paracetamol using the synthesis of GO was found to perform better at pH 7 and contact time of 80 minutes with GO from palm kernel shell as adsorbent. The adsorption was best described by the pseudo-second-order kinetic model and Freundlich isotherm. Therefore, the rind of orange and palm kernel shell can be used as low-cost adsorbents for the removal of paracetamol in solution. Further purification and modification of these GOs may be carried out to enhance their adsorptive capacity.

Conflicts of interest

The authors report there are no competing interests to declare.

Individual author's contributions

Conception: [TM]
Design: [TM]
Execution: [A]
Interpretation: [A]
Writing the paper: [TM & A]

References

Akhavan, O., Bijanzad, K., and Mirsepah, A. (2014). Synthesis of graphene from natural and Industrial carbonaceous wastes. In RSC Adv., 4, 20441-20448 https://doi.org/10.1039/C4RA01550A

Akpotu, S.O., and Moodley, B. (2018). Application of as-synthesised MCM-41 and MCM-41 wrapped with reduced graphene oxide/graphene oxide in the remediation of acetaminophen and aspirin from aqueous system Journal of Environmental Management 209: 205-215. doi.org/10.1016/j.jenvman.2017.12.037.

Alam, S.N., Sharma, N., and Kumar, L. (2017). Synthesis of Graphene Oxide (GO) by Modified Hummers Method and Its Thermal Reduction to Obtain Reduced Graphene Oxide (rGO). Graphene 6: 1-18. http://dx.doi.org/10.4236/graphene.2017.61001

Al-Khateeb, L.A. Almotiry, S., and Salam, M.A. (2014). Adsorption of pharmaceutical pollutants onto graphene nanoplatelets. Chemical Engineering Journal 248: 191- 199. doi.org/10.1016/j.cej.2014.03.023

Amir Faiz, M.S., Azurahanim, C., Yazid, Y., Suriani, A.B., and Ain, S.N. (2020). Preparation and characterization of graphene oxide from tea waste and it's photocatalytic application of TiO_2/graphene nano composite Materials Research Express 7,015613. doi.org/10.1088/2053-1591/ab689df

Aro-modiu, O., Osobamiro, M.T., and Osundeko, A.O. (2019). Synthesis and Characterization of Graphene Oxide from Agricultural Waste Scienta Africana, An International Journal of Pure & Applied Sciences 18: 143-151. ISSN 1118-1931.

Barroso, P.J., Santos, J.L., Martín, J., Aparicio, I., and Alonso, E. (2019). Emerging contaminants in the atmosphere: Analysis, occurrence and future challenges. Critical reviews in environmental science and technology 49:104–171. https://doi.org/10.1080/10643389.2018.1540761

Chen, H., Gao, B., and Li, H. (2015). Removal of sulfamethoxazole and ciprofloxacin from aqueous solutions by graphene oxide. Journal of Hazardous Materials, 282:201–207.DOI: 10.1016/j.jhazmat.2014.03.063

Debbarma, J., PeetamMandal, P., and Saha, M. (2020). Chemistry and Mechanism of One-Step Formation of Graphene from Agrowaste Letters in Applied Nano bioscience 9: 1389 – 1394. https://doi.org/10.33263/LIANBS93.13891394

Gao, Y., Li, Y., Zhang, L., Huang, H., Hu, J., Shah, S.M., and Su, X. (2012). Adsorption and removal of tetracycline antibiotics from aqueous solution by graphene oxide. Journal of Colloid and Interface Science 368: 540–546. DOI: 10.1016/j.jcis.2011.11.015

Grace, A.S., and Malar, G.S.P.L. (2020). Synthesis and Characterization of Graphene Oxide from Coconut Husk Ash, Oriental journal of chemistry 36: 348-352. http://dx.doi.org/10.13005/ojc/360220

Catherine, H.N., Ming-Han, O., Basavaraju, M., and Yang-hsin, S. (2018). Adsorption mechanism of emerging and conventional phenolic compounds on graphene oxide nanoflakes in water, Science of The Total Environment, 635: 629-638. 10.1016/j.scitotenv.2018.03.389

Homem, V., and. Santos, V. (2011). Degradation and removal methods of antibiotics from aqueous matrices — a review, J. Environ. Manage. 92: 2304–2347. DOI: 10.1016/j.jenvman.2011.05.023

Ismail, M., Weng, C.N., Rahman, H.A., and Zakaria, N.A. (2013). "Freundlich isotherm equilibrium equastions in determining effectiveness a low-cost absorbent to heavy metal removal in wastewater (leachate) at TelukKitang Landfill, Pengkalan Chepa, Kelantan, Malaysia Journal of Geography and Earth Science, 1: 01-08.

Li, X., Wang, Z., Li, Q., Ma, J. and Zhu, M. (2015). Preparation, characterization, and application of mesoporous silica-grafted graphene oxide for highly selective lead adsorption, Chemical Engineering Journal, 273: 630-637. 10.1016/j.cej.2015.03.104

Li, Y., Du, Q., Liu, T., Sun, J., Jiao, Y., Xia, Y., Xia, L., Wang, Z., Zhang, W., Wang, K., Zhu, H., and Wu, D. (2012). Equilibrium, kinetic and thermodynamic studies on the adsorption of phenol onto graphene Materials Research Bulletin, 47:1898–1904. https://doi.org/10.1016/j.materresbull.2012.04.021

Li, Y., Du, Q., Liu, T., Sun, J., Wang, Y., Wu, S., Wang, Z., Xia, Y., and Xia, L. (2013). Methylene blue adsorption on graphene oxide/calcium alginate composites, Carbohydrate polymers, 95: 501–507. DOI: 10.1016/j.carbpol.2013.01.094

Liu, X., Zhang, H., Ma, Y., Wu, X., Meng, L., Guo, Y., Yu, G., and Liu, Y. (2013). Graphene-coated silica as a highly efficient sorbent for residual organophosphorus pesticides in water, Journal of materials chemistry A, 1: 1875-1884. https://doi.org/10.1039/C2TA00173J

Macías-García, A., García-Sanz-Calcedo, J., Carrasco-Amador, J.B., and Segura-Cruz, R. (2019). Adsorption of Paracetamol in Hospital

Wastewater Through Activated Carbon Filters Sustainability 11: 2672 doi:10.3390/su11092672

Marcano, D.C., Kosynkin, D.V., Berlin, J.M., Sinitskii, A., Sun, Z., Slesarev, A., Alemany, L.B., Lu, W., and Tour, J.M. (2010). Improved synthesis of graphene oxide. ACS Nano, 4: 4806–4814. https://doi.org/10.1021/nn1006368

Moussavi, G., Hossaini, Z., and Pourakbar, M. (2016). Preparation, characterization and adsorption potential of the NH4Cl-induced activated carbon for the removal of amoxicillin antibiotic from water, Chemical Engineering Journal, 287: 665–673. DOI https://doi.org/10.1016/j.cej.2012.11.069

Mukoko, T., Mupa, M., Guyo, U., and Dziike, F. (2015). Preparation of Rice Hull Activated Carbon for the Removal of Selected Pharmaceutical Waste Compounds in Hospital Effluent, Journal of Environmental and Analytical Toxicology, 7: 2–9. DOI: 10.4172/2161-0525.S7-008

Nasir, S., Hussein, M.Z., Yusof, N.A., and Zainal, Z. (2017). Electrochemical Energy Storage Potentials of Waste Biomass: Oil Palm Leaf- and Palm Kernel Shell-Derived Activated Nanomaterials 7, 182. doi:10.3390/nano7070182

Rivera-Utrilla, J., Sánchez-Polo, M., Ferro-García, M.Á., Prados-Joya, G., and Ocampo-Pérez, R. (2013). Pharmaceuticals as emerging contaminants and their removal from water. A review Chemosphere 93: 1268–1287. https://doi.org/10.1016/j.chemosphere.2013.07.059

Shih, C., Lin, S., Sharma, R., Strano, M.S., and Blankschtein, D. (2012). Understanding the pH-Dependent Behavior of Graphene Oxide Aqueous Solutions: A Comparative Experimental and Molecular Dynamics Simulation Study Langmuir 28:235–241.https://doi.org/10.1021/la203607w

Somanathan, T., Prasad, K., Ostrikov, K.K., Saravanan, A., and Krishna, V.M. (2015). Graphene oxide Synthesis from Agro-waste Nanomaterials 5: 826-834. https://doi.org/10.3390/nano5020826.

Sui, Z.Y., Zhou, D., and Han, B.H. (2016). Fabrication of graphene-based porous materials and their applications in environmental fields. In Graphene Science Handbook. Applications and Industrialization; Edited by M. Aliofkhazraei, N. Ali, W.I. Milne, C.S. Ozkan, S. Mitura and J.L. Gervasoni, Springer, FL, 399–418. ISBN 9780429169359

Sun, Y., Yang, S., Zhao, G., Wang, Q., and Wang, X. (2013). Adsorption of polycyclic aromatic hydrocarbons on graphene oxides and reduced graphene oxides, Chemistry: An Asian Journal, 8: 2755–2761. https://doi.org/10.1002/asia.201300496

Tijani, J.O., Fatoba, O.O., Babajide, O.O., and Petrik, L.F. (2016). Pharmaceuticals, endocrine disruptors, personal care products, nanomaterials and perfluorinated pollutants: a review, Environmental chemistry letters, 14: 27–49. DOI 10.1007/s10311-015-0537-z

Tohamy, H-A.S., Anis, B., Youssef, M.A., Abdallah, A.E.M., El-Sakhawy, M., and Kamel, S. (2020). Preparation of eco-friendly graphene oxide from agricultural wastes for water treatment. Desalination and Water Treatment. 191: 250–262. doi: 10.5004/dwt.2020.25652

Wang, H., Yuan, X., Wu, Y., Huang, H., Zeng, G., Liu, Y., Wang, X., Lin, N., and Qi, Y. (2013). Adsorption characteristics and behaviours of graphene oxide for Zn (II) removal from aqueous solution, Applications of surface science, 279: 432–440. https://doi.org/10.1016/j.apsusc.2013.04.133

Yuan, G., Yan, L., Liang, Z., Hui, H., Junjie, H., Syed, M.S., and Xingguang, S. (2012). Calcined graphene/MgAl-layered double hydroxides for enhanced Cr (VI) removal, Journal of Colloid and Interface Science, 368: 540–546. DOI:10.1016/J.CEJ.2013.01.090

Zhang, Y.L., Zhang, J., Dai, C.M., Zhou, X.F., and Liu, S.G. (2013). Sorption of carbamazepine from water by magnetic molecularly imprinted polymers based on chitosan-Fe_3O_4. Carbohydrate polymers 97: 809–816. DOI: 10.1016/j.carbpol.2013.05.072

This journal is © The Nigerian Young Academy 2022